On the Cause of the 1930s Dust Bowl

Siegfried D. Schubert, Max J. Suarez, Philip J. Pegion , Randal D. Koster,
and Julio T. Bacmeister
Earth Sciences Directorate, NASA/GSFC
Greenbelt, Maryland

Popular Summary

The 1930s was characterized by a decade of rainfall deficits and high temperatures that desiccated much of the United States Great Plains. Numerous dust storms created one of the most severe environmental catastrophes in U.S. history and led to the popular characterization of much of the southern Great Plains as the "Dust Bowl". In this study, we show that the origin of the drought was in the anomalous tropical sea surface temperatures that occurred during that decade. We further show that interactions between the atmosphere and the land surface were essential to the development of the severe drought conditions. The results are based on simulations with the NASA Seasonal-to-Interannual Prediction Project general circulation model forced with observed and idealized sea surface temperatures. We contrast the 1930s drought with other major droughts of the 20th century, and speculate on the possibility of another Dust Bowl developing in the foreseeable future.

On the Cause of the 1930s Dust Bowl

Siegfried D. Schubert, Max J. Suarez, Philip J. Pegion[1], Randal D. Koster, and Julio T. Bacmeister[2]
Earth Sciences Directorate, NASA/GSFC
Greenbelt, Maryland

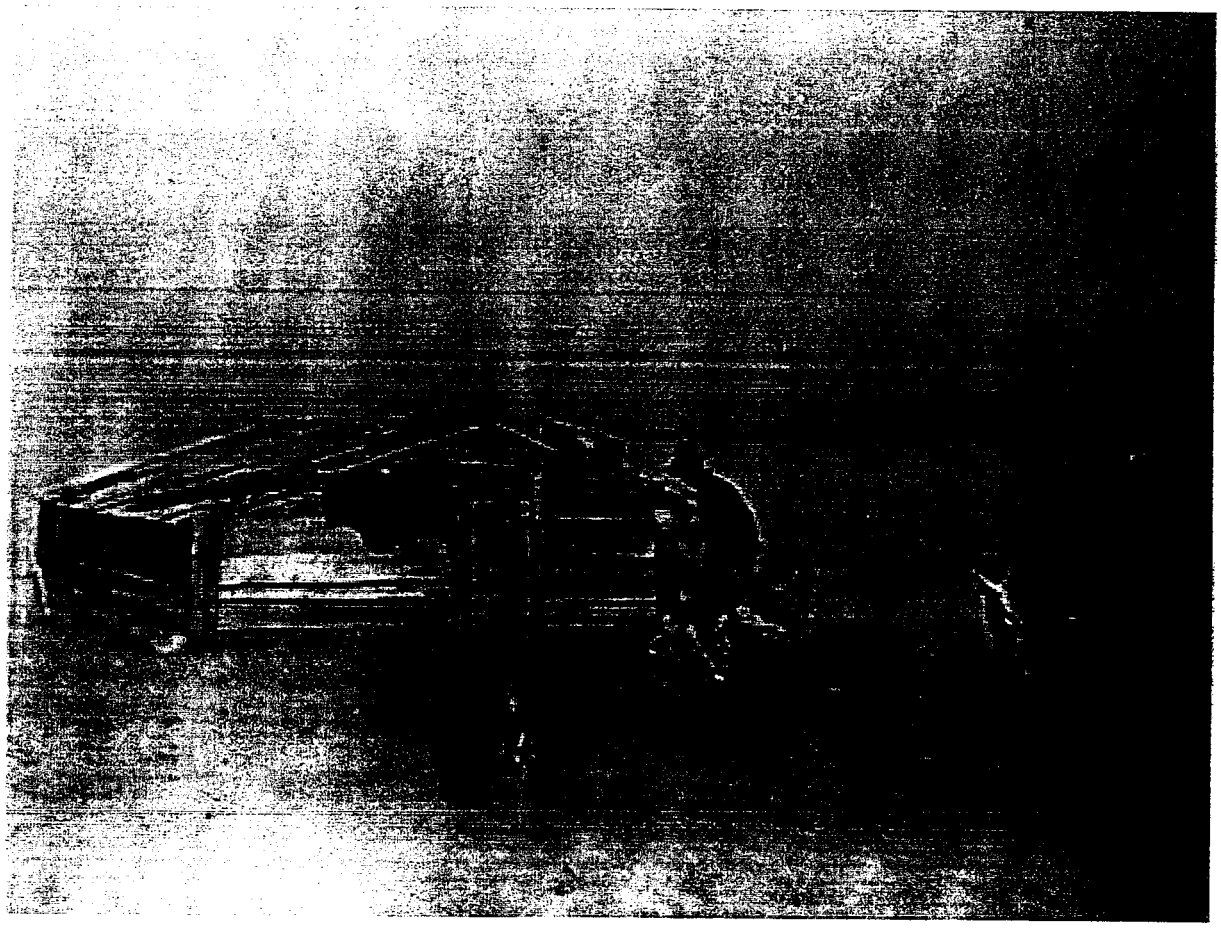

Dust Storm, Cimarron County, Oklahoma, 1936 (A. Rothstein, Library of Congress)

Manuscript to be submitted to

Science

---

[1] Additional affiliation: Science Applications International Corporation, Beltsville, Maryland
[2] Additional affiliation: Goddard Earth Sciences and Technology Center (GEST), University of Maryland, Baltimore, MD 21250

During the 1930s the United States experienced one of the most devastating droughts of the last century. The drought affected almost two-thirds of the country and parts of Mexico and Canada and was infamous for the numerous dust storms that occurred in the southern Great Plains – a region that became known as the "Dust Bowl". In this study, we show that the origin of the drought was in the anomalous tropical sea surface temperatures (SSTs) that occurred during that decade. We further show that interactions between the atmosphere and the land surface were essential to the development of the severe drought conditions. The results are based on simulations with the NASA Seasonal-to-Interannual Prediction Project general circulation model forced with observed and idealized sea surface temperatures. We contrast the 1930s drought with other major droughts of the 20th century, and speculate on the possibility of another Dust Bowl developing in the foreseeable future.

The 1930s was characterized by a decade of rainfall deficits and high temperatures that desiccated much of the United States Great Plains. Numerous dust storms created one of the most severe environmental catastrophes in U.S. history and led to the popular characterization of much of the southern Great Plains as the "Dust Bowl" (1).

While progress has been made in understanding some of the important processes contributing to drought conditions (e.g., 2,3,4,5,6), the mechanisms by which a drought can be maintained over many years have not been well established. A number of previous studies have used the historical record of meteorological and oceanographic observations to identify statistical relationships between slowly varying Pacific Ocean SSTs and precipitation over the Great Plains (7,8), though the record of observations is too short to provide definitive results for long-term drought. Understanding the causes of the 1930s drought is particularly challenging in view of the scarcity of upper-air meteorological observations prior to about 1950.

Several recent studies (9,10,11) have employed state-of-the-art atmospheric-land general circulation models (AGCMs) forced with observed sea surface temperatures to shed new light on the physical mechanisms the produce prolonged drought conditions. In one study (9), it was shown that recent unprecedented changes in the tropical oceans (the warming of the tropical Indian and western Pacific Oceans along with a cooling in the eastern tropical Pacific) contributed to the recent prolonged drought conditions that affected much of the northern middle latitudes. In another study (10), it was shown that multi-year drought in the Great Plains during the last 70 years is partly forced by a large-scale pattern of SST variability that spans much of the Pacific Ocean (hereafter referred to as the pan-Pacific pattern), though it is primarily the tropical part of the pattern that forces the droughts. That study further showed the importance of local land-atmosphere feedbacks in the development and maintenance of multi-year drought in the Great Plains. A third study (11) sheds new light on the causes of the severe drought conditions that occurred in the African Sahel region during the 1970s and 1980s. Those results, based on an analysis of the same AGCM simulations used in (10), demonstrated the importance of tropical SST anomalies in forcing long-term variations in the Sahel precipitation. That study also found that interactions with the land surface acted to amplify the Sahel drought conditions.

The current study is focused on the causes of the Dust Bowl drought. While (10) demonstrated the importance of the pan-Pacific SST pattern in forcing multi-year precipitation variations in the Great Plains, that particular SST pattern did not have unusually large amplitude during the 1930s. In fact, the SST anomalies were rather weak throughout the tropical Pacific during that decade. Our study is based on a number of century-long simulations carried out with the NASA Seasonal-to-Interannual Prediction Project (NSIPP) atmospheric-land general circulation model (12) - the same model that was used in (10), though run here at a somewhat coarser horizontal resolution (13). The basic model simulations considered here are an ensemble of fourteen 100-year (1902-2001) runs forced by observed monthly sea surface temperatures (14). These simulations will be referred to as the C20C runs, since they were carried out as part of the

Climate of the 20th Century project (15). The runs differ only in their initial atmospheric conditions. As such, the degree of similarity in the runs (the "signal") provides us with an assessment of how much the sea surface temperatures control Great Plains climate variations, while the disagreement among the runs (the "noise") provides us with an estimate of the unpredictable component of the climate variability.

We begin by presenting in Figure 1 time series of precipitation area-averaged over the Great Plains, together with maps of the precipitation anomalies time-averaged for the period 1932-38: the period encompassing the most severe drought conditions of that decade. Results are presented from observations (16) and from the fourteen simulations. The time series are filtered (17) to remove time scales shorter than about 6 years. The thin black curves show the individual ensemble members, the green curve is the ensemble mean., and the red curve is the observed rainfall. The time series of the observed and simulated anomalies show considerable variability, with extended periods of both above and below normal conditions throughout the century. The correlation between the observed and the ensemble mean anomalies is 0.57[3]. While there is considerable scatter among the ensemble members, there are periods during which all the curves tend to follow one another. In particular, during the 1930s Dust Bowl almost all of the runs show a tendency for dry conditions, consistent with the observations. The dry conditions of the 1930s are followed, in the early 1940s, by a rapid transition by all ensemble members to wetter conditions, again consistent with the observations. In general, the simulations agree with the observations to the extent that the observed anomalies fall within the scatter of the ensemble members. The mid 1970s show a rather peculiar result in that most of the runs indicate very dry conditions, while the observations and two of the ensemble members show a tendency for slightly wet or neutral conditions. This would suggest, if we believe the model results, that we were lucky to have had near normal conditions during the 1970s, since the probability of having a major drought was rather high (12 chances out of 14 or 86%). In fact, the historical tendency for droughts to occur in the Great Plains roughly every 20 years (1910s, 1930s, 1950s),

[3] For comparison, the correlation between the ensemble mean and the individual simulations ranges from 0.53 – 0.79.

together with the very dry conditions that existed over parts of the central U.S. by the mid-1970s, collectively led to considerable speculation at the time that we were about to enter an extended dry period (18,19).

Figure 1 also includes maps of the ensemble mean and observed precipitation anomalies averaged over the Dust Bowl period (1932-38). The observations show deficits exceeding 0.1 mm/day covering much of the central United States, with peak deficits exceeding 0.3 mm/day centered on Kansas. The simulated anomalies are similar to the observed with peak deficits of similar magnitude and again centered over Kansas. The main discrepancy is the large deficit simulated over Mexico that does not show up in the observations (20). The simulation also does not capture the full spatial extent of the drought, particularly the dry conditions that were observed over the northern Great Plains and parts of Canada. An inspection of the individual ensemble members shows that this discrepancy with the observations occurs as a result of the ensemble averaging which acts to filter out the unpredictable (noise) component of the simulated anomalies. In fact, there is a wide range in the spatial extent of the dry conditions among the ensemble members, with some showing negative precipitation anomalies (<-0.1) extending well into Canada and covering an area that exceeds that of the observed anomalies.

Figure 2 two shows the global SST anomalies (14) averaged over the Dust Bowl period. While these mean anomaly maps represent our best estimates of the SST during the 1930s, it must be emphasized that the fields are constructed from extrapolations of a rather limited number of ship observations employing modern-era statistical basis functions (14). Figure 2 shows that the anomalies are negative in most places including the tropical Pacific and North Pacific, as well as much of the Southern Ocean. Positive anomalies occur in the tropical and North Atlantic Oceans, as well as some regions of the South Pacific. The tropical anomalies tend to be small, with the absolute value of the anomalies generally less than 0.3°C. The largest anomalies occur in the North Atlantic and just off the coast of Asia centered on Japan, where anomalies exceed 0.5°C in absolute value.

In order to better understand the role of the SST anomalies, we carried out a number of idealized experiments in which the SST forcing was limited to various sub-regions (see outlines in Figure 2) and averaged over the 1932-38 Dust Bowl period. In particular, we are interested in separating the contributions from each of the three tropical basins and the extratropics. From the experiments summarized in Table 1, the impact of tropical Pacific SST anomalies was computed as (*Pacific-Control*). For the tropical Atlantic and Indian Oceans, the impact was computed as a difference between the run forced with the full tropical basin SSTs and a run *without* anomalies in that basin (*Atlantic* = *Tropical* - *PacInd* and *Indian* = *Tropical* – *PacAtl*). A similar approach was used to obtain the extratropical contribution. This residual approach to assessing the impact of regional anomalies was prompted by our prior experience with similar experiments using El Niño SST anomalies. In that case, the direct approach resulted in nonlinearities due to the large response to Pacific anomalies, particularly over North America. The residual approach used here to separate Indian, Atlantic, and extratropical responses ameliorates this effect.

Table 1: The idealized SST experiments. The anomalies are the time-averaged (1932-38) deviations from the 1902-1999 mean (21). All runs are 100 years in length. The regions are defined in Figure 2.

Run	**SST**
Control	Climatological (average of 1902-1999)
Global	Global anomalies
Tropical	Anomalies confined to tropics, climatological elsewhere
Pacific	Anomalies confined to tropical Pacific
PacAtl	Anomalies confined to tropical Pacific and tropical Atlantic
PacInd	Anomalies confined to tropical Pacific and tropical Indian Ocean
Fixed Beta	Global anomalies and atmosphere-land surface interaction disabled

We first examine whether forcing the model with the 1932-38 time-mean SST anomalies produces the same time mean response in the Great Plains precipitation as that obtained from the original

C20C (14-member ensemble) runs. The top two panels of Figure 3 compare the time-mean precipitation anomalies for 1932-38 from the C20C (ensemble mean) and *Global* runs. The results are quite similar. In addition to the dry anomalies, the idealized forcing also reproduces some of the wet anomalies in the Pacific Northwest and along the southeast coast. There are some discrepancies between the runs. Most notably, the rainfall deficits extend into Alabama in the *Global* run but are not in the C20C runs; similar discrepancies occur over the Pacific Northwest. Despite these minor differences between the results from the C20C and *Global* runs, it appears that the basic drought conditions that the model simulated in the Great Plains during the 1930s can be explained as a response to the time mean global SST anomalies. Details in the year-to-year variations of the SSTs in that decade played at most a secondary role in shaping the drought.

We next examine the influence of the time mean tropical SST alone (the *Tropical* run). The results (lower left panel of Figure 3) show that the main features of the drought conditions in the central and western Great Plains are reproduced with only the tropical SST forcing. The *Global minus Tropical* difference map (lower right panel) shows that the impact of the extratropical SSTs is to broaden the region of drought conditions especially to the east and south of the central Great Plains, and to increase the region of wet anomalies in the Pacific Northwest. We remind the reader that the extension of the drought into Alabama in the *Global* run (top right panel of Figure 3) did not occur in the C20C runs, and so we are led to conclude that that is an artifact of forcing the model with only the time mean SSTs, the same can be said for the extended wet conditions in the Pacific Northwest.

The remaining idealized SST runs attempt to separate the roles of the different ocean basins as discussed above. The results are summarized in Figure 4 where we now focus on the core Dust Bowl region (1). The first two points show that the observed and ensemble mean C20C precipitation anomalies are nearly the same. The large intra-ensemble spread of the C20C runs, however, indicates that the near equality of the two values is likely a fortuitous result. The

remaining points in Figure 4 show a repeat of the C20C ensemble mean value and the various 100-year mean values obtained from the idealized SST runs. The bars show the 90% confidence intervals.[4] The first two points to the right of the vertical dashed line show that the Dust Bowl precipitation anomaly produced in the *Global* run is statistically indistinguishable from that produced in the C20C run. The impact of the extratropics ("*Extratropics*" is defined as *Global minus Tropical*) on the Dust Bowl region is not significant. This is consistent with the fact that we cannot distinguish between the deficit produced in the *Global* and T*ropical* runs (the 90% confidence intervals overlap). The blue points show the impact of the combined basin runs (*PacInd* and *PacAtl*), and the yellow points are our estimates of the separate contributions from the three tropical ocean basins (*Pacific*, *"Atlantic"*defined as *Tropical minus PactInd*, and *"Indian"*defined as *Tropical minus PactAtl)*. The results show that only the contributions from the Pacific and Atlantic Oceans are significant, though the 90% confidence intervals are quite large so that very little can be said about the relative contributions of the tropical basins to the total tropical response. This is highlighted by the large confidence intervals attached to the *Tropical Sum* defined as *Pacific plus "Atlantic" plus "Indian"*.

The green (*Fixed Beta*) point in Figure 4 is the result of repeating the *Global* run, but in this case disabling the interactions between the atmosphere and land surface (22). Comparing those results with the results from the *Global* run, we see that the impact of not allowing land-atmosphere interactions is to reduce the precipitation deficit by 50%. The much tighter confidence intervals associated with the *Fixed Beta* results show that disabling the interactions with soil moisture results in much less precipitation variability, consistent with previous studies employing the same model (6,10). Figure 5 compares the precipitation anomaly maps for the *Global* and *Fixed Beta* runs. Clearly, the Dust Bowl region shows much reduced precipitation deficits in the run

[4] The confidence intervals are computed assuming that the annual mean precipitation anomalies come from a normal distribution. For the C20C result, the variance estimates required to compute the t-values come from the 14 ensemble members, while for the idealized SST runs the variance is estimated from the 100 years assuming independence of the annual mean anomalies.

without land-atmosphere feedbacks. These results are consistent with previous work (6) that shows that the Great Plains region is particularly sensitive to soil moisture changes.

The results presented so far have been for annual mean conditions, though it is well known that most of the rain in the Great Plains tends to fall during the spring and summer seasons. We show in Figure 6 the seasonal distribution of the observed area-averaged precipitation anomalies together with those from the *Global* run. We also include for comparison the *Fixed Beta* run. The results from the *Global* run are quite similar to the observed, though there is a general tendency to underestimate the deficits. The largest deficits occur during the warm season, with about half the deficit occurring during the summer months. Somewhat surprisingly, the fall season has larger deficits than the spring season. The winter season precipitation anomalies are by comparison rather small; in fact, the observed winter anomaly is slightly positive. The main impact of disabling the interactions with the land surface is to dramatically reduce the deficit during JJA. The seasonality of the spatial distribution of the observed and simulated Great Plains precipitation anomalies (not shown) is also similar. The largest differences occur during spring, when the ensemble mean simulated drought is confined to the southern tier of states, while the observations show the drought extending much further north to cover most of the central United States.

The results of our model simulations provide compelling evidence that the 1930s tropical SST anomalies forced changes in the atmospheric circulation that, together with local land-atmosphere interactions, produced one of the most devastating droughts to occur in the United States during the last century. Both the tropical Pacific and tropical Atlantic Ocean basins appear to play a role. The deficit obtained as a contribution from the tropical Indian Ocean basin was found to be not statistically significant (using 90% confidence intervals). An analysis of the circulation changes (not shown) suggests that the role of the cold Pacific SST anomalies was to generate a global-scale response in the upper troposphere (negative height anomalies in the tropics and a tendency for positive height anomalies in the middle latitudes) that suppresses rainfall over the

Great Plains. The warm Atlantic SST anomalies produced two upper level anticyclonic circulation anomalies on either side of the equator with the northern anomaly extending across the Gulf of Mexico and the southern United States. In the lower troposphere, the response to the warm Atlantic SST anomalies was a cyclonic circulation anomaly that was positioned to suppress the supply of moisture entering the continent from the Gulf of Mexico. It is noteworthy that the Atlantic response is confined almost exclusively to the summer and fall season.

While the severity, extent, and duration of the 1930s drought was unusual for the 20th century, proxy climate records indicate that major droughts have occurred in the Great Plains approximately once or twice a century over the last 400 years (23). There is evidence for multi-decadal droughts during the late thirteenth and sixteenth centuries that were of much greater severity and duration than those of the 20th century (23). For example, tree ring analyses in Nebraska suggest that the drought that began in 1276 lasted 38 years (24).

An analysis of the other major central U.S. droughts of the 20th century (10) suggests that the SST anomalies that produced the Dust Bowl were rather unique (cool tropical Pacific Ocean together with a warm Atlantic Ocean), though it must be pointed out that a cool tropical Pacific Ocean appears to be a common factor in all the major droughts of the 20th century. Figure 1 shows that since the early 1980s (but with the exception of 1987-89), the Great Plains generally experienced above normal precipitation. On the other hand, during the last five years much of the western (especially the southwestern) United States, including some parts of the Great Plains, has experienced below normal precipitation leading to moderate to extreme drought conditions[5]. The cause of this primarily western U.S. drought is unclear though a preliminary look at the relationship between SSTs and long-term precipitation variations over the southwestern United States from our C20C runs suggests a strong link to the pan-Pacific pattern discussed earlier in

[5] See the NOAA drought monitoring page (http://lwf.ncdc.noaa.gov/oa/climate/research/drought).

connection with Great Plains drought. One difference compared with the Great Plains is that the southwestern United States appears to have a stronger link to the Indian Ocean SSTs.

A key question is, of course, whether we should expect another "Dust Bowl" in the near future. While the exact distribution of the SSTs that led to the Dust Bowl may be rather rare, and there is no evidence to suggest that we are about to enter another period with such an SST configuration, there are certainly other patterns of tropical SST anomalies that can lead to multi-year drought in the Great Plains (e.g., 7, 8, 10). Having said that, we must point out that the current generation of coupled atmosphere-ocean models do not provide skillful predictions of the tropical oceans on time scales longer than about a year. In addition, the potential role of global warming during the recent decades further complicates the picture by making it difficult to apply the lessons learned from the analysis of earlier (pre-industrial) droughts. The development of improved coupled models and an improved understanding of the nature and role of global warming are essential ingredients for making progress on the drought prediction problem.

Acknowledgements: This work was supported by the NASA Earth Science Enterprise's Global Modeling and Analysis Program, and the NASA Seasonal-to-Interannual Prediction Project.

References and notes

1. D. Worster, *Dust Bowl: The Southern Great Plains in the 1930s.* Oxford University Press, New York, 277 pp. (1979). The "Dust Bowl" was loosely defined to be the region encompassing the western third of Kansas, Southeastern Colorado, the Oklahoma Panhandle, the northern two-thirds of the Texas Panhandle, and Northeastern New Mexico.

2. Namias, J., 1955: Some meteorological aspects of drought with special reference to the summers of 1952-1954 over the United States. Mon.Wea.Rev., 83, 199-205.

3. Trenberth, K.E., G.W. Branstator and P.A. Arkin, 1988: Origins of the 1988 North American drought. Science, 242, 1640-1645.

4. Atlas, R., N. Wolfson and J. Terry, 1993: The effect of SST and soil moisture anomalies on the GLA model simulations of the 1988 U.S. drought. J. Climate, 6, 2034-2048.

5. Mo, K.C., J. Nogues-Paegle, and R.W. Higgins, 1997: Atmospheric processes associated with summer floods and droughts in the central United States. J.Climate Sci., 10, 3028-3046.

6. Koster R.D., M.J. Suarez, M. Heiser, 2000: Variance and predictability of precipitation at seasonal-to-interannual timescales. J. Hydrometeor., 1, 26-46.

7. Ting, M. and H. Wang, 1997: Summertime U.S. precipitation variability and its relation to Pacific Sea Surface Temperature, J. Climate, 10,1853-1873.

8. Barlow, M., S. Nigam, and E.H. Berbery, 2001: ENSO, Pacific Decadal Variability, and U.S. summertime precipitation, drought, and streamflow. J. Climate, 14, 2105-2128.

9. Hoerling, M.P. and A. Kumar, 2003: The perfect ocean for drought. Science, 299, 691-699.

10. Schubert, S. D., M.J. Suarez, P. Pegion, R.D. Koster, and J.T. Bacmeister, 2003: Causes of long-term drought in the United States Great Plains. J. Climate, conditionally accepted.

11. Giannini, A., R. Saravanan, and P. Chang, 2003: Oceanic forcing of Sahel rainfall on interannual to interdecadal timescales. Accepted for publication in Science.

12. Bacmeister, J., P.J. Pegion, S. D. Schubert, and M.J. Suarez, 2000: An atlas of seasonal means simulated by the NSIPP 1 atmospheric GCM, NASA Tech. Memo. No. 104606, volume 17, Goddard Space Flight Center, Greenbelt, MD 20771, 2000.

13. The model was run with a 3 ° latitude by 3.75° longitude horizontal grid compared with a 2 ° latitude by 2.5 ° longitude grid in the earlier study (13). The resolution change was made for computational efficiency, and does not appear to have much impact on the basic model climatology or variability.

14. Rayner, N.A., D.E. Parker, E.B. Horton, C.K. Folland, L.V. Alexander, D.P. Rowell, E.C. Kent, and A. Kaplan, 2003: Global analyses of sea surface temperature, sea ice and night marine air temperature since the late nineteenth century, *J. Geophys. Res.*, 108(D14), 4407, doi:10.1029/2002JD002670.

15. WMO, 2001: Report of the sixteenth session of the CAS/JSC Working Group on Numerical Experimentation. *WMO TD 1076*

16. Vose,R., R. Schmoyer, P. Steurer, T. Peterson, R. Heim, T. Karl, and J. Eischeid, 1992: *The Global Historical Climatology Network: long-term monthly temperature, precipitation, sea level pressure, and station pressure data.* ORNL/CDIAC-53, NDP-041. Carbon Dioxide Information Analysis Center, Oak Ridge National Laboratory, Oak Ridge, Tennessee.

17. The filter is described in Zhang, Y., J.M. Wallace, and D. Battisti, 1997: ENSO-like interdecadal variability: 1900-93. J. Climate, 10, 1004-1020.

18. J.R. Borchert, *The Dust Bowl in the 1970's.* Assoc.Amer.Geogr.Ann., **61**, 1-22 (1971).

19. N. Rosenberg, Introduction to *North American Droughts.* AAAA Selected Symposia Series. Westview Press, Boulder Colorado, N.J. Rosenberg, Ed., pp 1-7 (1978)

20. Mexico experienced on-average somewhat above normal precipitation during the 1930s. This appears to be in part due to a number of hurricanes that made landfall over Mexico especially

during 1933 and 1936. In fact the entire decade of the 1930s was marked by above normal hurricane activity in the Atlantic. The coarse resolution of the model runs precludes the simulation of hurricanes and this may account for some of the unrealistic dry conditions simulated by the model over Mexico.

21. The SSTs actually used to force the model have the time mean shown in Figure 2, however, the anomalies where computed separately for each calendar month. Specifically, the SSTs were computed for each calendar month as the sum of a mean annual cycle (computed for the period 1902-1999) and the SST anomaly field for that calendar month.

22. We turn off the interaction between the land and atmosphere by fixing the evaporation efficiency or "β" (ratio of the evaporation to the potential evaporation) in the land surface model formulation to its seasonal climatology, as described in (6). Here the potential evaporation is the maximum rate at which the atmosphere can receive water (as controlled by near-surface humidity gradients, wind speed etc.). We note that this version of the NSIPP model uses specified, but seasonally varying, vegetation cover so we cannot examine the impact of any changes to the vegetation.

23. C.A. Woodhouse, J.T. Overpeck, *Bull.Amer.Meteor.Soc.*, **79**, 2693-2714 (1998).

24. D.L. Bark, History of American Droughts. *North American Droughts.* AAAA Selected Symposia Series. Westview Press, Boulder Colorado, N.J. Rosenberg, Ed., pp 9-23 (1978)

List of Figures

Figure 1: Time series of precipitation anomalies averaged over the United States Great Plains region (30°-50°N, 95°-105°W, see box in insets). A filter is applied to remove time scales shorter than about 6 years. The thin black curves are the results from the fourteen ensemble members produced with the NSIPP-1 model forced by observed SST. The green solid curve is the ensemble mean. The red curve shows the observations. The maps show the simulated (left) and observed (right) precipitation anomalies averaged over the "Dust Bowl" time period (1932-38). Units: mm/day.

Figure 2: The global SST anomalies for the period 1932-1938. The boxes delineate the various sub-regions (tropical oceans, Indian Ocean, Pacific Ocean, Atlantic Ocean) used in designing the idealized SST forcing experiments. The anomalies are the differences from the 1902-1999 climatology based on the HADISST dataset. Units: °C.

Figure 3: Top left panel: ensemble mean precipitation anomalies averaged for the period 1932-1938 from the C20C runs. Top right panel: The 100-year mean precipitation anomalies from the idealized forcing experiment where the atmosphere is forced with the global distribution of the time mean HadISST anomalies (see Figure 2 and Table 1). Bottom left panel: same as top right panel except that the SST forcing is confined to the tropics. Bottom right panel: The difference between the global SST anomaly and tropical SST anomaly runs. Units: mm/day. In all but the C20C panel, values are shaded only if they are significant at the 10% level based on a t-test. The contour intervals are the same as the shading intervals (see color bar) with dashed contours indicating negative values.

Figure 4: The precipitation anomalies averaged over the Dust Bowl region (36°N-39°N, 99.5°W-105°W) for the period 1932-1938. The first two points compare the observed and C20C results (the bar denotes the ensemble spread measured by +/- one standard deviation). Points to the right of the dashed vertical line show the results from the various idealized SST runs and a repeat of the

C20C value. Here the bars denote the 90% confidence intervals. See text for details. Units are mm/day.

Figure 5: Top panel: The 100-year mean precipitation anomalies from the run forced with the global distribution of the 1932-38 SST anomalies (see Figure 2 and Table 1). Lower right panel: Same as top panel accept for the run with the global SST anomalies and fixed beta (no atmosphere-land surface interaction). Units are mm/day. Shading indicates significance at the 10% level based on a t-test. The contour intervals are the same as the shading intervals (see color bar) with dashed contours indicating negative values.

Figure 6: The observed (black bars) and simulated (gray bars) seasonal variation of the 1932-1938 mean precipitation anomalies averaged over the United States Great Plains (see box in inset in Figure 1). The light gray bars are for the run forced with the 1932-38 time-mean global SST. The dark gray bars are for the run also forced with the 1932-38 time-mean global SST, but with the interaction with soil moisture disabled (the fixed beta run, see text). The Units are mm/day. The labels on the abscissa indicate the seasons where DJF is December, January, February; MAM is March, April, May; JJA is June, July, August; SON is September, October, November. Note that for DJF, the fixed beta run produces anomalies that are too small to show up in the figure.

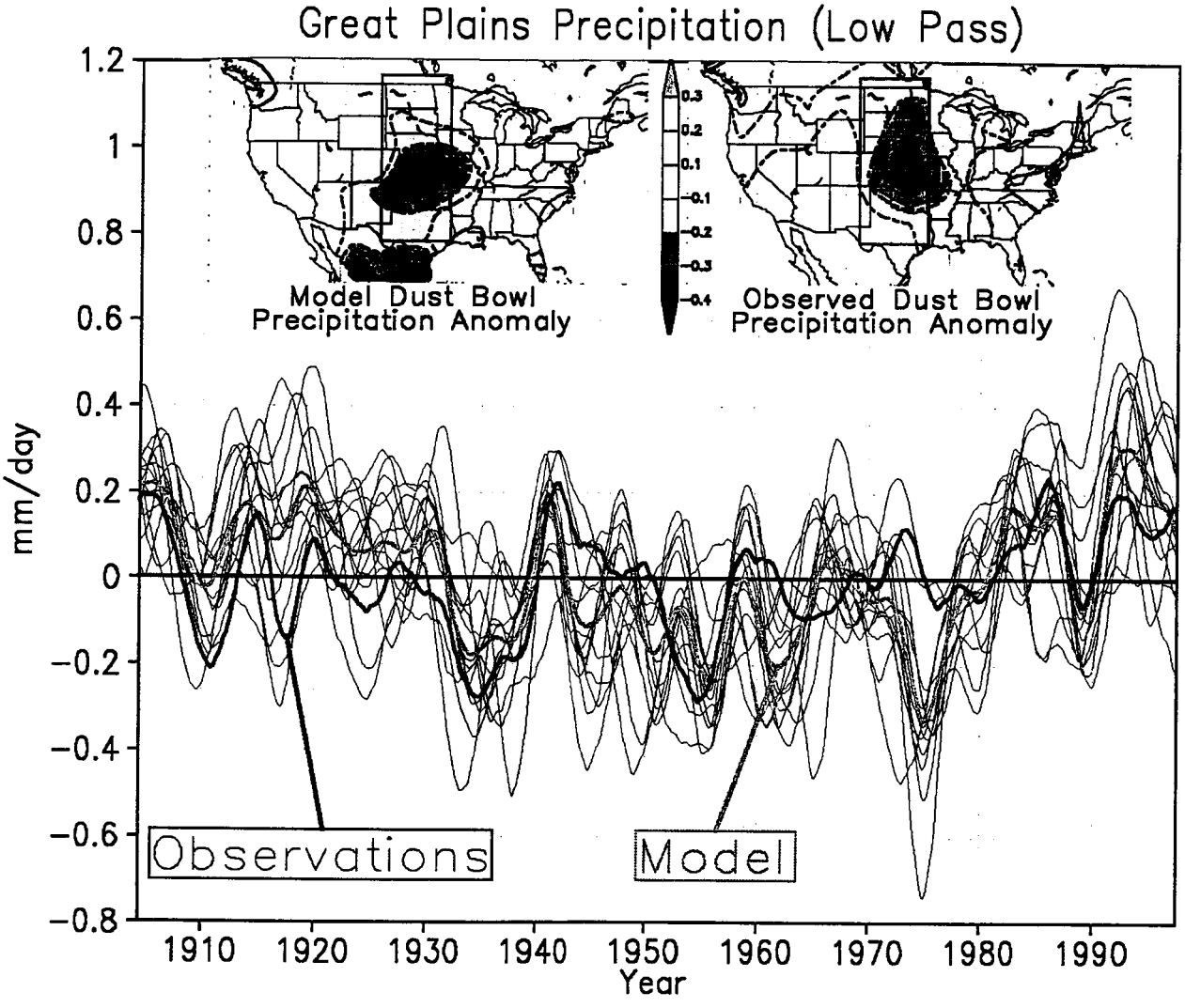

Figure 1: Time series of precipitation anomalies averaged over the United States Great Plains region (30°-50°N, 95°-105°W, see box in insets). A filter is applied to remove time scales shorter than about 6 years. The thin black curves are the results from the fourteen ensemble members produced with the NSIPP-1 model forced by observed SST. The green solid curve is the ensemble mean. The red curve shows the observations. The maps show the simulated (left) and observed (right) precipitation anomalies averaged over the "Dust Bowl" time period (1932-38). Units: mm/day.

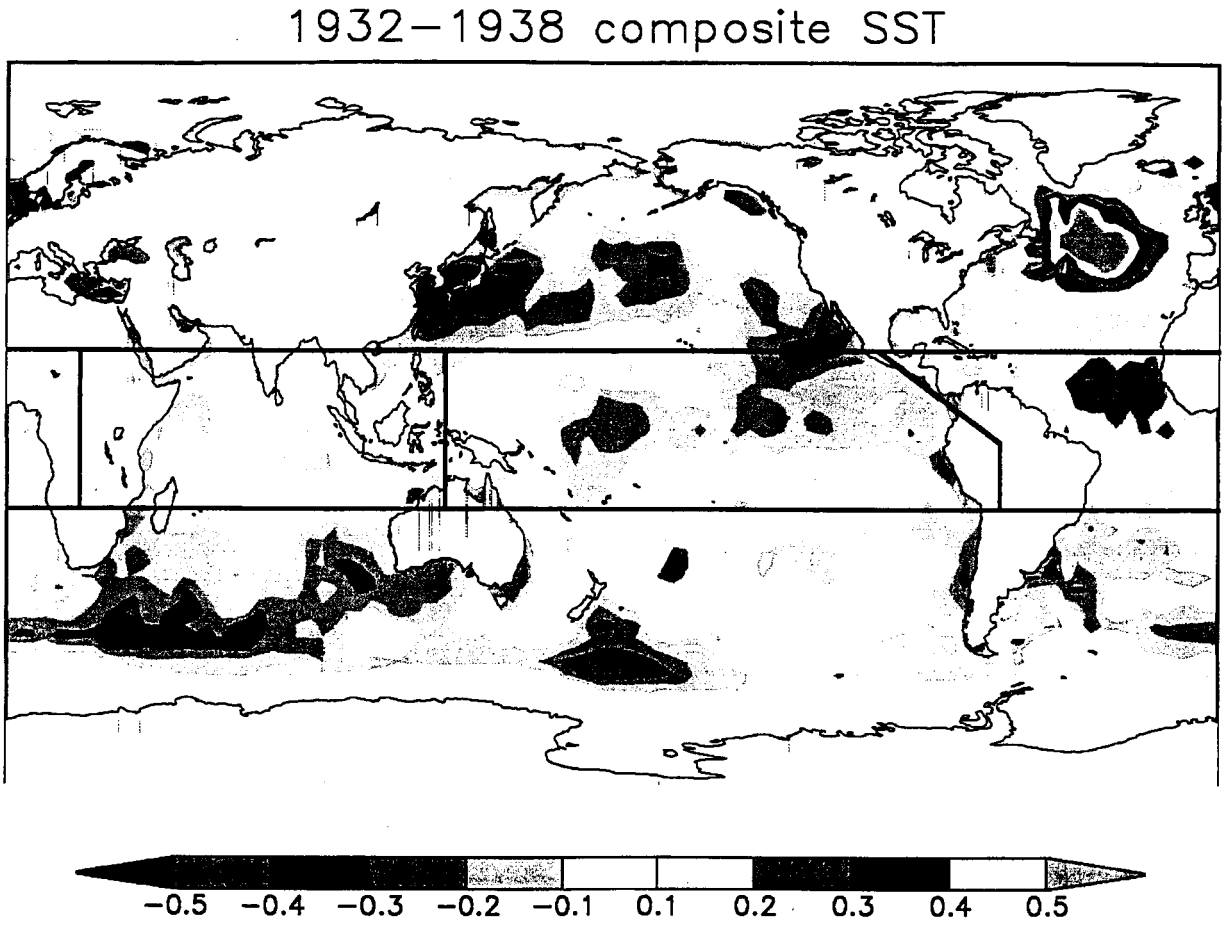

Figure 2: The global SST anomalies for the period 1932-1938. The boxes delineate the various sub-regions (tropical oceans, Indian Ocean, Pacific Ocean, Atlantic Ocean) used in designing the idealized SST forcing experiments. The anomalies are the differences from the 1902-1999 climatology based on the HADISST dataset. Units: °C.

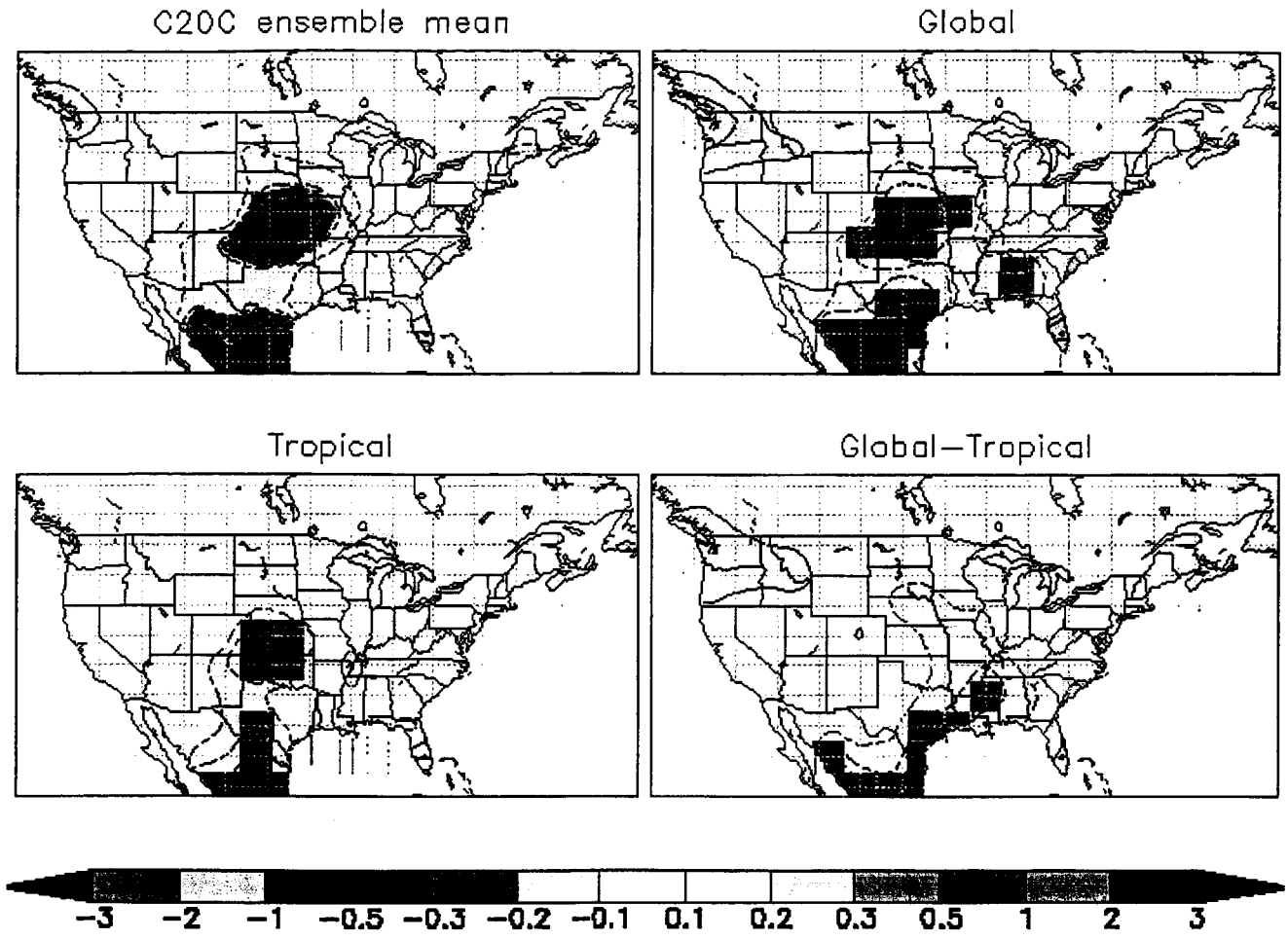

Figure 3: Top left panel: ensemble mean precipitation anomalies averaged for the period 1932-1938 from the C20C runs. Top right panel: The 100-year mean precipitation anomalies from the idealized forcing experiment where the atmosphere is forced with the global distribution of the time mean HadISST anomalies (see Figure 2 and Table 1). Bottom left panel: same as top right panel except that the SST forcing is confined to the tropics. Bottom right panel: The difference between the global SST anomaly and tropical SST anomaly runs. Units: mm/day. In all but the C20C panel, values are shaded only if they are significant at the 10% level based on a t-test. The contour intervals are the same as the shading intervals (see color bar) with dashed contours indicating negative values.

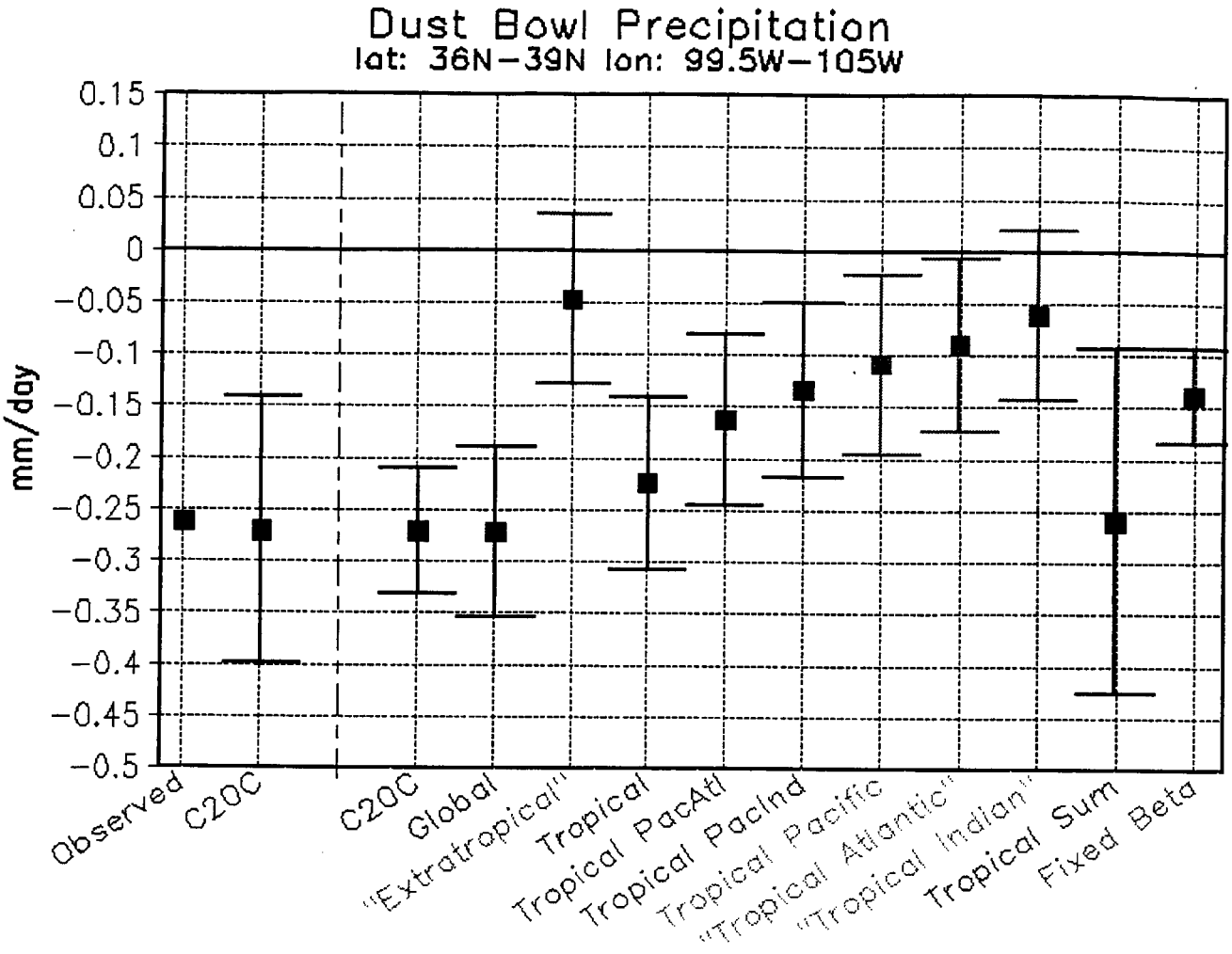

Figure 4: The precipitation anomalies averaged over the Dust Bowl region (36°N-39°N, 99.5°W-105°W) for the period 1932-1938. The first two points compare the observed and C20C results (the bar denotes the ensemble spread measured by +/- one standard deviation). Points to the right of the dashed vertical line show the results from the various idealized SST runs and a repeat of the C20C value. Here the bars denote the 90% confidence intervals. See text for details. Units are mm/day.

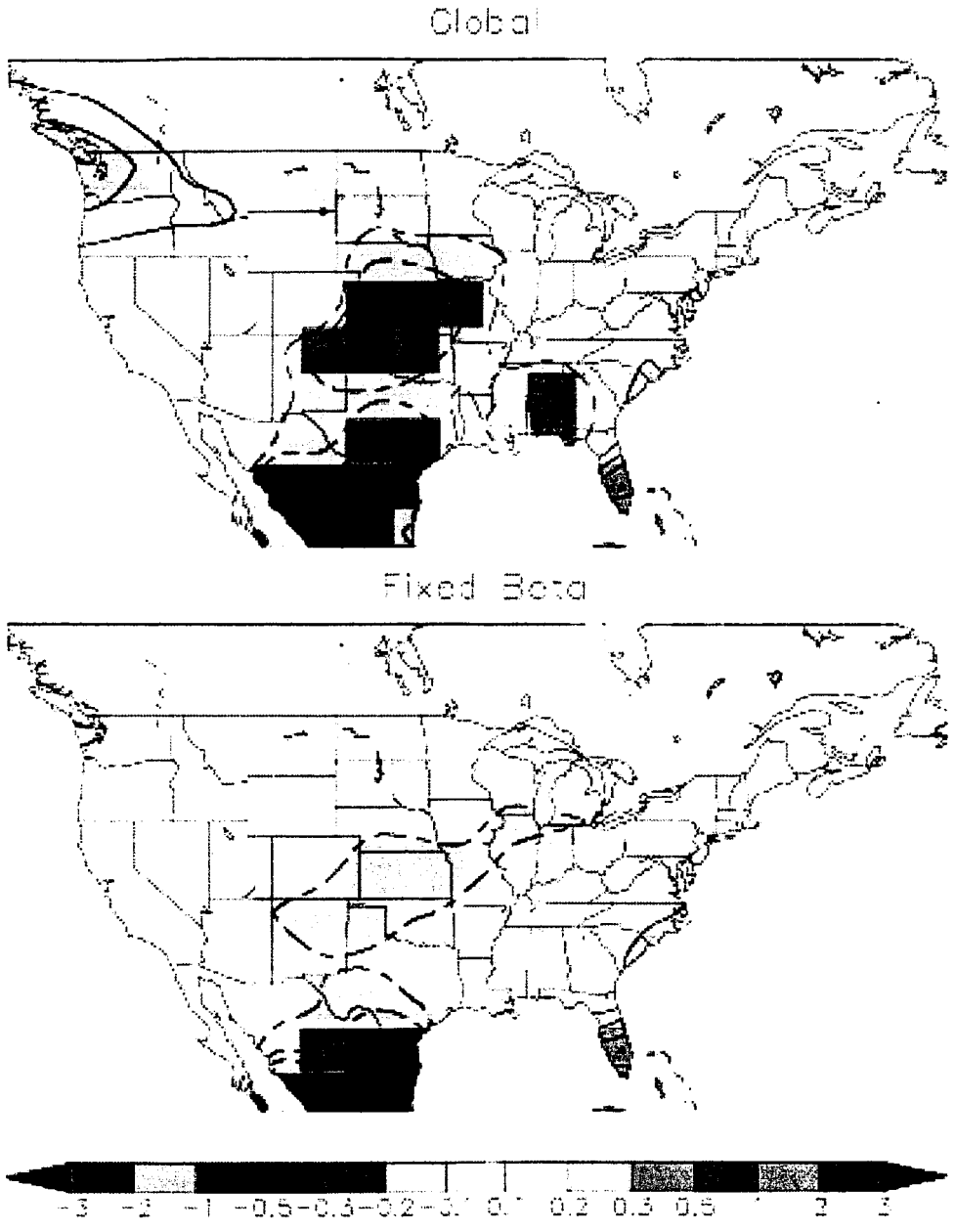

Figure 5: Top panel: The 100-year mean precipitation anomalies from the run forced with the global distribution of the 1932-38 SST anomalies (see Figure 2 and Table 1). Lower right panel: Same as top panel accept for the run with the global SST anomalies and fixed beta (no atmosphere-land surface interaction). Units are mm/day. Shading indicates significance at the 10% level based on a t-test. The contour intervals are the same as the shading intervals (see color bar) with dashed contours indicating negative values.

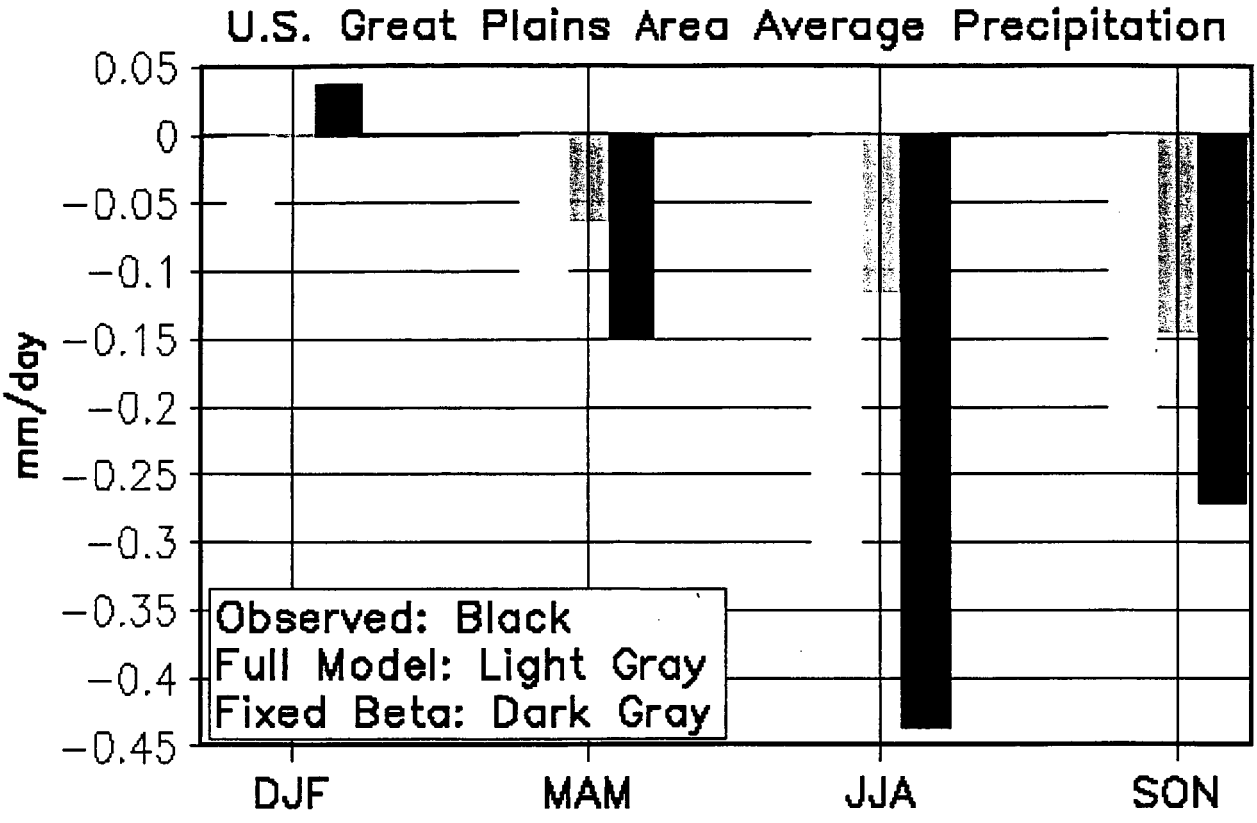

Figure 6: The observed (black bars) and simulated (gray bars) seasonal variation of the 1932-1938 mean precipitation anomalies averaged over the United States Great Plains (see box in inset in Figure 1). The light gray bars are for the run forced with the 1932-38 time-mean global SST. The dark gray bars are for the run also forced with the 1932-38 time-mean global SST, but with the interaction with soil moisture disabled (the fixed beta run, see text). The Units are mm/day. The labels on the abscissa indicate the seasons where DJF is December, January, February; MAM is March, April, May; JJA is June, July, August; SON is September, October, November. Note that for DJF, the fixed beta run produces anomalies that are too small to show up in the figure.